Nonlocal theory for heat transport at high frequencies

Yee Kan Koh,[1,2] David G. Cahill,[2] and Bo Sun[1]
[1]*Department of Mechanical Engineering, National University of Singapore, Singapore*
[2]*Department of Materials Science and Engineering, and Frederick Seitz Materials Research Laboratory, University of Illinois, Urbana, Illinois 61801, USA*
(Received 23 July 2013; published 11 November 2014)

We develop a nonlocal theory for heat conduction under high-frequency temperature fields and apply the theory to explain reductions of the apparent thermal conductivity observed in recent experiments. Our nonlocal theory is an analytical solution of the Boltzmann transport equation for phonons in a semi-infinite solid, similar to a prior nonlocal theory for heat conduction under a high-temperature gradient but subjected to periodic heating at the surface. The boundary condition of periodic heating, as opposed to prior calculations of heating by a single laser pulse, better mimics time-domain thermoreflectance (TDTR) and broadband frequency-domain thermoreflectance (BB-FDTR) measurements. We find that, except for pure crystals at high frequencies, the effective thermal conductivity derived using the nonlocal theory compares well with calculations of a modified Callaway model that includes an upper limit on the phonon mean-free path at twice the thermal penetration depth. For pure crystals, however, the effective thermal conductivity derived from the out-of-phase calculations are independent of frequency, in agreement with prior TDTR measurements, due to the countereffect of reduced heat flux and diminished relative phase between the heat flux and temperature oscillations at high frequencies. Our results suggest that empirical interpretation of ballistic phonons not contributing to heat conduction is not general and can only be applied to measurements on alloys and not pure crystals, even when a large laser spot size is used in the experiments and the interfacial thermal resistance is negligible.

DOI: 10.1103/PhysRevB.90.205412 PACS number(s): 63.20.dd, 44.05.+e, 72.15.Eb

I. INTRODUCTION

On large length scales, thermal energy transport in solids is governed by Fourier's law of heat conduction, $J = -\Lambda(\partial T/\partial x)$, where J is the heat flux, Λ is the thermal conductivity and $\partial T/\partial x$ is the temperature gradient. Fourier's law is a local theory: heat transport depends only on the material properties and temperature gradient at a single point in space, and is not affected by properties and temperature profiles at other locations. The validity of a local theory breaks down, however, when a significant portion of heat carriers is not in equilibrium with other heat carriers and thus is not driven by the local temperature gradient. A notable example of the violation of a local theory, which has been extensively investigated experimentally [1–5] and theoretically [6–10], is ballistic energy transport by nonequilibrium phonons, observed in nanostructures with characteristic lengths shorter than phonon mean-free-paths. Another example of breakdown of the local theory is transient cooling under a large temperature gradient (e.g., generated by laser pulses), when phonon mean-free paths are long compared to the length scale over which the temperature gradient changes. In this case, the measured [11] and calculated [12–14] heat flux is found to be smaller than predictions made using the local theory.

In principle, ballistic phonon transport can also occur for heat conduction at high oscillation frequencies, in which the characteristic lengths (i.e., the thermal penetration depths, $\boldsymbol{d} = \sqrt{\Lambda/(\pi C f)}$., where C is the volumetric heat capacity and f is the frequency of the oscillating temperature field) can be shorter than the mean-free paths ($\boldsymbol{\ell}$) of the dominant heat carriers. In fact, recent experiments [15–18] indicate that the apparent thermal conductivity of crystalline alloys and a particular form of amorphous Si is reduced from the steady-state values when an oscillating temperature field of MHz frequency is used in measurements. We previously attributed [15] this finding to the fact that long-wavelength phonons are not in equilibrium and traverse ballistically across the penetration depth ($\boldsymbol{\ell} > \boldsymbol{d}$), and thus do not contribute to the apparent thermal conductivity measured by TDTR. We thus proposed that the frequency dependence of thermal conductivity can be applied as a convenient probe [15] of the mean-free paths of phonons in alloys and amorphous Si.

For pure crystals, however, an apparent discrepancy is observed between prior measurements of Si by time-domain thermoreflectance (TDTR) as a function of modulation frequency and broadband frequency-domain thermoreflectance (BB-FDTR). Using BB-FDTR, the thermal conductivity of Si at 10 MHz is reduced [18] by >30%, but using TDTR, the measured thermal conductivity is independent [15] of modulation frequency within a frequency range of $0.1 < f < 10$ MHz. If our prior empirical interpretation [15] were correct, since $\boldsymbol{d} = 1.7\,\mu$m at 10 MHz, this lack of frequency dependence of the TDTR measurement of Si suggests that phonons with $\boldsymbol{\ell} > 1.7\,\mu$m do not contribute significantly to heat conduction in Si; this conclusion is inconsistent with recent first-principle calculations [19,20]. To address this discrepancy, Mingo *et al.* [21] suggested that the reduction in the measured thermal conductivity could instead be due to insensitivity of TDTR measurements to phonons with $\boldsymbol{\ell}_{\text{anh}} > 3\boldsymbol{d}$, where $\boldsymbol{\ell}_{\text{anh}}$ is the mean-free path of phonons due to anharmonic scattering only. Their calculations using the fitted cutoff of $3\boldsymbol{d}$ agree well with the frequency-dependent TDTR measurements.

Wilson and Cahill [22] posited that the reduced apparent thermal conductivity in the through-plane direction of semiconductor alloys is due to an inhomogeneous effective thermal conductivity near the surface of the samples that is

caused by the reflection and transmission of long mean-free-path phonons at the interface. However, rather than using a nonlocal model for thermal transport to directly predict the frequency-domain thermal response, they instead used a nonlocal model to derive effective thermal conductivities, and then used the effective thermal conductivities to generate the frequency-domain thermal response.

Wilson and Cahill [23] have also proposed a two-channel model capable of explaining the frequency dependence of the apparent thermal conductivity derived from TDTR measurements in terms of an interfacial nonequilibrium thermal resistance. While the two-channel model provides insight into the effect that different thermal boundary conditions have on the heat carried near the surface by different groups of phonons, it does not include nonequilibrium effects that result from shortened length scales; furthermore, dividing the spectrum of phonons into only two groups is a large simplification. The Boltzmann transport equation was solved by Minnich *et al.* [13,14] to investigate the suppression of apparent thermal conductivity measured by TDTR for small laser spot sizes and high frequencies; these authors applied, however, a simplified boundary condition (heating by a single pulse) that does not fully capture the physics of TDTR measurements, see the discussion in Sec. III.

In this paper, we provide a theoretical framework to predict when the effective thermal conductivity is reduced at high frequencies of oscillating temperature fields. We develop a nonlocal theory for heat conduction at high frequencies, and apply the nonlocal theory to a semi-infinite solid periodically heated at the surface. We assume negligible interfacial thermal resistance at the surface and calculate the heat flux by both ballistic and diffusive phonons from this approximation to the Boltzmann transport equations. We compare calculations of the nonlocal theory to calculations of a modified Callaway model that excludes either ballistic ($\ell > 2d$) or harmonic ($\ell_{\text{anh}} > 3d$) phonons. We find that for alloys, the suppression of the apparent thermal conductivity at high frequencies is due to reduced heat flux by nonequilibrium phonons, and this nonlocal effect can be approximately reproduced. For crystals at high frequencies, however, the effective thermal conductivity derived from the temperature oscillations that are 90° out of phase with the heat source are essentially independent of the heating frequency. This result is consistent with prior TDTR measurements that found the apparent thermal conductivity of Si to be independent of frequency and thus cannot be approximated by calculations of the Callaway model that omit ballistic phonons with an empirical $\ell > 2d$ cutoff. Our results provide insights for understanding thermal conductivity measurements by TDTR [15] and BB-FDTR [18].

The paper is organized as follows. In Sec. II, we adapt the time-domain nonlocal theory by Mahan and Claro [12] to develop a nonlocal theory for heat conduction under high-frequency heating. We derive an expression for heat flux by nonequilibrium phonons that depends on a weighted average of temperature gradients as a function of the depth from the surface. In Sec. III, we discuss the physical meanings of TDTR and BB-FDTR measurements and thus establish a correct form of boundary conditions for our nonlocal model to meaningfully represent the TDTR and BB-FDTR measurements. In our implementation of the nonlocal model, we apply the numerical schemes as summarized in Sec. IV and a modified Callaway model as discussed in Sec. V. In Sec. VI, we compare the predictions using the nonlocal theory to calculations by the modified Callaway model, using exactly the same distribution of phonon mean-free paths. We summarize our findings in Sec. VII.

II. FORMULATION OF THE NONLOCAL THEORY FOR HEAT TRANSPORT AT HIGH FREQUENCIES

To develop a nonlocal theory for heat conduction at high heating frequencies, we build on a nonlocal theory [12] developed by Mahan and Claro for heat conduction with large thermal gradients and heat fluxes, and consider a semi-infinite solid being heated periodically in time at the surface ($z = 0$) at frequency f; see Fig. 1. We only focus on understanding the frequency dependence of the thermal conductivity with large laser spot sizes, and do not attempt to address the dependence of the apparent thermal conductivity on finite laser spots observed by Minnich *et al.* [24]. Under such conditions, the heat flow is primarily one dimensional [22].

We assume that heat is carried in the semi-infinite solid predominantly by acoustic phonons, which are only partially in equilibrium with other phonons as a result of the high frequency of the heat source. Thus, to derive the population of (and subsequently the heat flux by) the acoustic phonons, we need to solve the Boltzmann transport equation for each phonon mode,

$$\frac{\partial N_q}{\partial t} + v_q \cdot \nabla N_q = -\frac{N_q - N_q^0}{\tau_q} \tag{1}$$

where the subscript q denotes each phonon mode with frequency ω and polarization j, N is the phonon distribution function, $N^0 = k_B T/\hbar\omega$ is the Planck distribution at high temperatures, τ is the total relaxation time of phonons, v is the phonon group velocity, $\hbar$ is the reduced Planck constant, and k_B is the Boltzmann constant.

To simplify and solve the Boltzmann transport equation [Eq. (1)], we assume that heat flow is one dimensional in the z direction and define $m = \cos\theta$, where θ is the angle between the z axis and phonon wave vector; see Fig. 1. We also define a pseudotemperature for the nonequilibrium phonons, $T_q^P = N_q \hbar\omega/k_B$; the pseudotemperature $T_q^P(z,t,m,q)$ is a function of position z, time t, direction m, and phonon mode q. Since we only consider periodic heating of $f < 100$ MHz, the relaxation time of the dominant heat carrying phonons in most materials, τ ($<10^{-9}$ s), is much shorter than $1/(2\pi f)$. Thus we ignore the time-dependent term in Eq. (1). This assumption is consistent with our previous assertion [15] that the reduction of the thermal conductivity of semiconductor alloys at heating frequencies <20 MHz is primarily an effect of length scales, i.e., mean-free paths and thermal penetration depths, and not an effect of time scales, i.e., phonon lifetimes and the period of the modulated heat source.

We performed the following calculation to confirm that the omission of the time-dependent term does not create significant error. We assume that the error of this omission is on the order of $\phi = 2\pi f\tau$ for each phonon mode with $\tau(\omega) < 1/(2\pi f)$ and on the order of unity ($\phi = 1$) for each

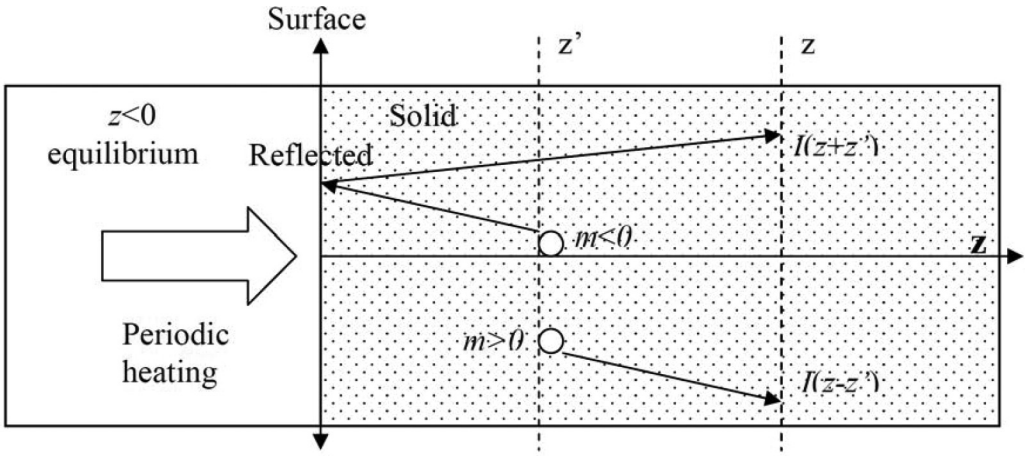

FIG. 1. An illustration of a semi-infinite solid ($z > 0$) being periodically heated on the surface ($z = 0$). We assume that phonons in $z < 0$ are all in equilibrium with Planck distribution within the time scale of interest. The circles represent two heat-carrying phonons with $m < 0$ and $m > 0$; the arrows represent the hypothetical phonon trajectory. $I_j(|z - z'|)$ represents the percentage of flux of unscattered phonons reaching z directly from z'; $I_j(|z + z'|)$, represents the percentage of flux of unscattered phonons reaching z from z' via reflection at the surface.

phonon mode with $\tau(\omega) > 1/(2\pi f)$. The overall error is then calculated by weighting the error for each mode by the thermal effusivity $\sqrt{\Lambda(\omega)C(\omega)}$ of that mode. (TDTR essentially measures the thermal effusivity of the samples; see Sec. III.) Thus, we estimate the error incurred by the omission as $\sum_j \int \sqrt{\Lambda(\omega)C(\omega)}\phi(\omega)d\omega / \sum_j \int \sqrt{\Lambda(\omega)C(\omega)}d\omega$, integrated over all the phonons in our modified Callaway model (see Sec. V) and summed over all polarizations j. The uncertainty is only $\sim$3% at $f = 100$ MHz and $\sim$1% at $f = 20$ MHz, for the hypothetical Si with $\Gamma = 2 \times 10^{-4}$ and $\Gamma = 2$ that we consider in Sec. V.

Applying the simplifications described above to Eq. (1), we derive

$$T_q^P + v_q m \tau_q \frac{\partial T_q^P}{\partial z} = T. \tag{2}$$

$T(z,t)$ is the equilibrium temperature at position z and time t, and is defined as the average of $T_q^P(z,t,m,q)$ for all phonons.

Equation (2) is an inexact first-order ordinary differential equation [25] that can be solved analytically. Applying the boundary conditions $T_q^P(0,t,m,q)$ and $T(0,t)$ at $z = 0$, the solution [12] of Eq. (2) gives

$$T_q^P(z,t,m,q) = T(z,t) + \exp\left(-\int_0^z \frac{dz'}{v_q m \tau_q(z',t,q)}\right)\left[T_q^P(0,t,m,q) - T(0,t)\right] - \int_0^z dz' \frac{\partial T(z',t)}{\partial z'} \exp\left(-\int_{z'}^z \frac{dz''}{v_q m \tau_q(z'',t,q)}\right), \tag{3}$$

where z' and z'' are variables of integration.

The pseudotemperature of the phonon modes at $z = 0$, $T_q^P(0,t,m,q)$ in Eq. (3), is not known and needs to be determined. Since $T_q^P(0,t,m,q)$ depends on many factors (e.g., transmission and scattering of phonons at boundaries, and coupling between phonons), we do not attempt to derive a general expression for $T_q^P(0,t,m,q)$. Instead, we propose a simple and convenient form of T_q^P that gives a physically meaningful solution to Eq. (2). For this purpose, we separately consider phonons that propagate to the surface ($m < 0$) and from the surface ($m > 0$) [12]. For the backward propagating phonons ($m < 0$), the exponential expression in the second term of Eq. (3) approaches infinity at large z. In order to have the second term of Eq. (3) vanish so that T_q^P remains finite, we follow Mahan and Claro [12] and choose

$$T_q^P(0,t,m,q) = T(0,t) + \int_0^\infty dz' \frac{\partial T(z',t)}{\partial z'} \exp\left(\frac{a_q(z',t,q)}{m}\right) \quad (m < 0), \tag{4a}$$

where $a_q(z,t,q) = \int_0^z \frac{dz''}{v_q \tau_q(z'',t,w)}$ is the distance z from the surface normalized by the mean-free paths $\ell_q(T,q) = v_q \tau_q$ of phonons. Substituting Eq. (4a) into Eq. (3), we derive an expression for $T_q^P(0,t,m,q)$,

$$T_q^P(z,t,m,q) = T(z,t) + \int_z^\infty dz' \frac{\partial T(z',t)}{\partial z'} \exp\left(-\frac{a_q(z,t,q) - a_q(z',t,q)}{m}\right) \quad (m < 0). \tag{4b}$$

To derive an expression for phonons that propagate away from the surface (forward propagating phonons, $m > 0$) using an assumption that physically represents the TDTR and BB-FDTR experiments, we assume that the semi-infinite solid is coated with a thin layer of metal at $z < 0$, with phonons in the metal layer always in thermal equilibrium. We further assume that

the interfacial thermal resistance of the metal/solid interface is negligible and thus all phonons from the metal transmit across the interface without being scattered. In such a scenario, the principle of detailed balance dictates that the average number of phonons of ω at $z = 0$ (including both phonons with $m < 0$ and $m > 0$) is given by the Planck distribution. Then, using Eq. (4) for phonons with $m < 0$, we derive the pseudotemperature T_q^P for $m > 0$ as

$$T_q^P(0,t,m,q) = T(0,t) - \int_0^\infty dz' \frac{\partial T(z',t)}{\partial z'} \exp\left(-\frac{a_q(z',t,q)}{m}\right) \quad (m > 0), \tag{5a}$$

$$T_q^P(z,t,m,q) = T(z,t) - \int_0^z dz' \frac{\partial T(z',t)}{\partial z'} \exp\left(-\frac{a_q(z,t,q) - a_q(z',t,q)}{m}\right) - \int_z^\infty dz' \frac{\partial T(z',t)}{\partial z'} \exp\left(-\frac{a_q(z,t,q) + a_q(z',t,q)}{m}\right) \quad (m > 0). \tag{5b}$$

Note that while Eq. (4) is similar to Eqs. (12) and (13) in Ref. [12], Eq. (5) is new and not previously derived.

Using the expressions for $T_q^P(z,t,m,q)$ in Eqs. (4) and (5), we derive a new expression for one-dimensional (1D) heat flux in the semi-infinite solid by nonequilibrium phonons, $J(z,t)$. We start with expressing $J(z,t)$ by counting the total heat carried by all phonon modes of three polarizations j,

$$J(z,t) = \sum_j \int \frac{d^3q}{(2\pi)^3} v_q \frac{\hbar\omega}{\exp\left(\hbar\omega/k_B T_q^P\right) - 1}. \tag{6}$$

For simplicity, we assume a truncated linear dispersion [15] for phonons, and include only acoustic phonons with frequency below a cutoff frequency ω_0^j for polarization j; ω_0^j is estimated from the Brillouin-zone boundary. Details of this modified Callaway model are given in Sec. V. Using this scheme, we only include ≈10% of total available phonon modes in the calculations [26], and implicitly assume that acoustic phonons near the Brillouin zone and optical phonons only significantly contribute to heat capacity but not heat transport. We assume that all phonons considered in the model travel at the speed of sound. As we did in solving the Boltzmann transport equation, we assume that temperatures are sufficiently high for all phonons ($k_B T_q^P \gg \hbar\omega$); by calculating the thermal conductivity of Si with and without the high-temperature assumption, we estimate that the error induced by this assumption is ∼13%. We also assume small perturbations ($T_q^P \approx T$ at all locations z), so that ℓ_q is independent of z and t and $a_q(z,t,q) = z/\ell_q$. Then, $J(z,t)$ becomes

$$J(z,t) = -\sum_j \frac{\left(\omega_0^j\right)^3 k_B}{24\pi^2 v_j^2} \int_0^\infty dz' \frac{\partial T(z',t)}{\partial z'} \times \left[I_j(|z - z'|) + I_j(|z + z'|)\right], \tag{7}$$

where the subscript j represents the polarization of phonons and $I_j(z)$ is the percentage of flux of unscattered phonons after the phonons traverse a normalized distance of $z/m\ell$,

$$I_j(z) = \frac{6}{\left(\omega_0^j\right)^3} \int_0^{\omega_0^j} \omega^2 d\omega \int_0^1 m dm \quad \exp\left(-\frac{|z|}{v_j m \tau}\right). \tag{8}$$

When $z/m\ell \approx 0$, $I_j(z) \approx 100\%$, i.e., most phonons remain unscattered when the distance traversed is small compared to the mean-free paths of the phonons ℓ. On the other hand, when $z/m\ell \gg 1$, $I_j(z) \approx 0$, i.e., most phonons are scattered when the distance traversed is much larger than the mean-free paths of the phonons ℓ.

We obtain the derivative of $J(z,t)$ with respect to distance z by differentiating Eq. (7),

$$\frac{\partial J(z,t)}{\partial z} = -\sum_j \frac{\left(\omega_0^j\right)^3 k_B}{24\pi^2 v_j^2} \int_0^\infty dz' \frac{\partial^2 T(z',t)}{\partial z'^2} \times \left[I_j(|z - z'|) - I_j(|z + z'|)\right]. \tag{9}$$

Our Eqs. (7) and (9) are similar to Eq. (19) in Ref. [12], but are more general. In Ref. [12], the authors assumed a simplified expression for the relaxation times right from the beginning of their derivation and thus the derived heat flux is only valid for the assumed relaxation times. By contrast, Eqs. (7) and (9) are general for any expressions of relaxation times within the framework of the relaxation time approximation (RTA), which can be readily incorporated into our nonlocal model. Also, we derive Eqs. (7) and (9) from realistic boundary conditions, while in Ref. [12], the boundary conditions were arbitrarily applied for the sake of convenience. Last, but importantly, we express Eqs. (8) and (9) in a physically meaningful form that can be simplified to the Fourier's law in the limit of low heating frequency, as discussed below. For example, our $I_j(z)$ represents a percentage of unscattered phonons, but in Ref. [12] $I(u)$ is a mathematical expression with limited physical meaning.

It is interesting to note that starting from an approximation to the Boltzmann transport equation for nonequilibrium phonons, we derive an expression for heat flux that depends not only on the local temperature gradient, but also on temperature gradients at all locations; see the integral in Eq. (7). To further elucidate this point, consider the heat flux at a location z in the semi-infinite solid; see Fig. 1. According to the nonlocal theory described by Eq. (7), heat flux is proportional to the weighted average of temperature gradients. The integrand in Eq. (7) is the product of the temperature gradient, $\partial T/\partial z'$, at point z', and a weighting term $I_j(|z - z'|) + I_j(|z + z'|)$, representing the percentage of the flux of phonons that remain unscattered after traveling directly from z to z', $I_j(|z - z'|)$, or artificially through reflection at the surface, $I_j(|z + z'|)$, as illustrated in Fig. 1. We emphasize that the reflection at the surface does not physically occur, but instead is a result of the phonon exchange that we assume at the interfaces. Due to the weighting term,

heat flux is only sensitive to $\partial T/\partial z'$ at a location close to z, in which $I_j(|z-z'|) \gg 0$ or equivalently $|z-z'| \approx \ell$.

We consider solving the temperature profile of the semi-infinite solid subjected to periodic heating of frequency f at the surface using Eq. (7). At low f, $\partial T/\partial z'$ within $|z-z'| \sim \ell$ is approximately constant for dominant heat-carrying phonons, and thus the integrand converges to the local temperature gradient, i.e., Fourier's law. At high f, however, $\partial T/\partial z'$ within the distance $|z-z'| \sim \ell$ changes substantially, and thus the contribution of temperature gradients from other locations cannot be ignored. The reduction of heat flux due to the nonlocal effect is discussed in Sec. VI.

III. EFFECTIVE THERMAL CONDUCTIVITIES AND HIGH-FREQUENCY LIMITS OF TDTR AND BB-FDTR MEASUREMENTS

Finally, we derive the effective thermal conductivity at high frequencies by solving the corresponding heat flux and temperature oscillations on the surface of the semi-infinite solid ($z = 0$) using the nonlocal theory. The derived effective thermal conductivities are intended to provide insights into TDTR and BB-FDTR measurements.

In the experiments, the structure of a typical sample is a metal film transducer, with a thickness on the order of 100 nm, deposited on top of the sample under study. Unfortunately, due to this two-layer structure, quantitative comparison between calculations of the nonlocal theory and the measurements requires a method for taking into account the thermal mass of the transducer (layer 1) and the thermal conductance of the interface between the transducer and the sample (layer 2). In the limit of high modulation frequencies ($f \gg \Lambda/(C \cdot w_0^2)$, where w_0 is the $1/e^2$ radius of the laser beams), and taking into account that $\Lambda_1/L_1 \gg G$ in most experiments, the weighted average of the temperature distribution [27] measured in the frequency domain by the probe beam can be approximated as

$$\Delta T(f) = \frac{P}{\pi w_0^2}\left(\frac{1/\gamma_2 + 1/G}{1 + i2\pi f C_1 L_1 (1/G + 1/\gamma_2)}\right), \quad (10)$$

where P is the amplitude of the absorbed heat, G is the thermal conductance of the interface between layer 1 and layer 2, L_1 is the thickness of the metal transducer, and the thermal conductivity Λ_n, and $\gamma_n = \sqrt{i2\pi f C_n \Lambda_n}$ are properties of layer n.

In TDTR measurements, the frequency components picked up by the lock-in amplifier are at $m/\tau \pm f$, where m is an integer, $1/\tau$ is the laser repetition rate, and f is the modulation frequency [27]. We further assume that the modulation frequency f is sufficiently low that $f < G^2/(2\pi\Lambda_2 C_2)$ and the thermal conductance is moderately low so that $G < \sqrt{2\pi\Lambda_2 C_2/\tau}$ (i.e., for Si, $f = 10\,\text{MHz}$ and $G = 200\,\text{MW m}^{-2}\,\text{K}^{-1}$ can simultaneously satisfy both conditions) and Eq. (10) can be further simplified. We then approximate the in-phase (V_{in}) and out-of-phase (V_{out}) signals picked up by the rf lock-in amplifier in TDTR measurements [27] as

$$\begin{aligned} V_{\text{in}} &= A\sum_{m=-\infty}^{\infty}[\Delta T(m/\tau + f) + \Delta T(m/\tau - f)\exp(i2\pi m t/\tau)], \\ V_{\text{out}} &= -iA\sum_{m=-\infty}^{\infty}[\Delta T(m/\tau + f) - \Delta T(m/\tau - f)\exp(i2\pi m t/\tau)], \\ \Delta T(m/\tau \pm f) &= \frac{P}{\pi w_0^2\sqrt{i2\pi f \Lambda_2 C_2}} \quad \text{if} \quad m = 0 \\ &= \frac{P}{\pi w_0^2}\left(\frac{1}{G + i2\pi(m/\tau \pm f)C_1 L_1}\right) \quad \text{if} \quad m \neq 0, \end{aligned} \quad (11)$$

where A is a proportionality constant independent of frequency.

Since $f \ll m/\tau$ in TDTR measurements for all terms except $m = 0$, first-order expansion of terms with $m/\tau \pm f$ in Eq. (11) leads to linear terms containing $(1 \mp \frac{f}{m/\tau})$. Thus, for V_{in}, the $\pm f$ terms cancel due to the infinite summation of $\Delta T(\frac{m}{\tau} + f)$ and $\Delta T(\frac{m}{\tau} - f)$ and only real terms at frequencies of m/τ remain. In the time domain, this corresponds to in-phase temperature decay at the sample surface after being heated by a train of *unmodulated* laser pulses at a repetition rate of $1/\tau$. For high thermal conductivity substrates such as Si, the temperature decay is mainly governed by the thermal conductance of the transducer/metal interfaces as well as the heat capacitance of the transducer layer as indicated by the ΔT expression in Eq. (11). As a result, in-phase TDTR signals are primarily used to derive G. On the other hand, V_{out} is dominated by two imaginary terms at frequency f and $-f$ after the infinite summation in Eq. (11). In the time domain, this corresponds to out-of-phase temperature oscillations induced by sinusoidal, *continuous* heating at the modulation frequency f. Thus, in TDTR, the thermal conductivity is derived predominantly from the out-of-phase temperature response at f, not from cooling of the sample surface after being heated by a single laser pulse, as commonly misunderstood and previously applied [13,14].

For BB-FDTR measurements, the thermal conductivity is derived from the phase shift (ϕ) between the periodic heating and the temperature oscillations at the sample surface. To correlate the measured ϕ to the temperature oscillations ($\Delta T_S = |\Delta T_{\max}|e^{i\theta_S}$) in the substrate that we calculate in this

paper, we substitute $\gamma_2 = |\gamma_2|e^{i\theta_2}$ in Eq. (10) and derive

$$\phi = \phi_1 - \phi_2,$$
$$\phi_1 = \tan^{-1}\left(\frac{-\sin(\theta_2)/|\gamma_2|}{1/G + \cos(\theta_2)/|\gamma_2|}\right), \quad (12)$$
$$\phi_2 = \tan^{-1}\left(\frac{2\pi f C_1 L_1 [1/G + \cos(\theta_2)/|\gamma_2|]}{1 + 2\pi f C_1 L_1 \sin(\theta_2)/|\gamma_2|}\right),$$

where ϕ_1 is the phase of the numerator and ϕ_2 is the phase of the denominator in Eq. (10).

When heat conduction obeys the Fourier's law, θ_2 is always $\pi/4$. If the frequency f is sufficiently small, the phase shift can be simplified as $\phi = -\frac{\pi}{4} + \frac{\gamma_2}{\sqrt{2}G} - \sqrt{\frac{\pi f C_1^2 L_1^2}{C_2 \Lambda_2}}$, the phase shift measured by BB-FDTR is not a constant even under the Fourier's law due to the thermal mass of the transducer layer. When the nonlocal theory of heat conduction is applied to the substrate, the phase in the substrate (θ_S) is no longer $-\pi/4$. The phase ϕ can still be calculated using Eq. (12) by substituting $\cos(\theta_2)/|\gamma_2|$ in the equation with in-phase response of the temperature oscillation in the substrate calculated using the nonlocal theory and substituting $\sin(\theta_2)/|\gamma_2|$ with the out-of-phase response. Thus, ϕ depends on both the in-phase and out-of-phase of the temperature oscillations in the substrate, in a rather complicated manner.

In this paper, we intend to understand the frequency dependence of the apparent thermal conductivity measured by TDTR and BB-FDTR through calculations of the temperature responses in the substrate using the derived nonlocal theory of heat conduction. In our calculations, we apply either a periodic heat flux or a periodic temperature oscillation at the surface of the semi-infinite solid, and monitor the corresponding temperature oscillation or heat flux. If Fourier's law of heat conduction is obeyed, the corresponding amplitudes of the heat flux and temperature on the surface $J_{\max}$ and $\Delta T_{\max}$ are related by $\frac{J_{\max}}{\Delta T_{\max}} = \sqrt{2\pi f C \Lambda}$. We thus define an effective thermal conductivity (Λ_{amp}) from the amplitude of the oscillations; see Eq. (13a). Λ_{amp}, however, is not very useful to understand TDTR and BB-FDTR measurements, because, as explained earlier, TDTR is sensitive to out-of-phase response while BB-FDTR is sensitive to both in-phase and out-of-phase responses. We thus define two additional effective thermal conductivities from the out-of-phase (Λ_{out}) and in-phase (Λ_{in}) of the calculated temperature oscillations,

$$\Lambda_{\text{amp}} = (J_{\max}/\Delta T_{\max})^2/(2\pi f C), \quad (13a)$$
$$\Lambda_{\text{out}} = \Lambda_{\text{amp}}/(2\sin^2\phi), \quad (13b)$$
$$\Lambda_{\text{in}} = \Lambda_{\text{amp}}/(2\cos^2\phi), \quad (13c)$$

where ϕ is the phase between the heat flux and temperature in the substrate. We compare these effective thermal conductivities to calculations of a modified Callaway model (see Sec. V) to provide insights to the frequency dependence of the apparent thermal conductivity measured by TDTR and BB-FDTR.

IV. NUMERICAL IMPLEMENTATION SCHEME

Since the heat flux equation is nonlocal and cannot be solved analytically, Λ_{amp}, Λ_{out}, and Λ_{in} can only be derived numerically. We thus discretize a semi-infinite solid using a graded mesh and numerically solve Eqs. (7) and (9) for the semi-infinite solid using a fully implicit scheme. We truncate the semi-infinite solid at $z = 10\boldsymbol{d}$, where $\boldsymbol{d}$ is the thermal penetration depth. Since the exact temperature oscillations after $10\boldsymbol{d}$ are not important, we approximate the temperature oscillations at $10\boldsymbol{d}$ using the analytical classical solution [28],

$$\Delta T = J_{\max}\exp(-x/d) \times \cos(2\pi f t - \pi/4 - x/d)/\sqrt{2\pi f C \Lambda_{SS}}, \quad (14)$$

where Λ_{SS} is the thermal conductivity of bulk solids under a steady-state condition. To improve computational efficiency of our numerical model, we discretize the semi-infinite solid using a graded mesh for $z < 5\boldsymbol{d}$ and a uniform mesh for $z > 5\boldsymbol{d}$; see Fig. 2. With the graded mesh, finer meshes are applied to regions where the temperature gradient is steeper and thus the accuracy of our computation is improved with the same amount of computation effort. We set the size of the first control volume (labeled "0") as $\Delta z_0/2$, and the size of the subsequent nth control volume as $\Delta z_n = \Delta z_0 r^n$ for $n < N_1$, where N_1 is the total number of control volumes in $z < 5\boldsymbol{d}$. The constant r is set to ensure that the size of the N_1th and $(N_1 + 1)$th elements are identical. For $5\boldsymbol{d} < z < 10\boldsymbol{d}$, the sizes of the control volumes are uniform and given by $\Delta z_i = 5\boldsymbol{d}/N_2$, where N_2 is the total number of control volumes in $5\boldsymbol{d} < z < 10\boldsymbol{d}$. We ensure that a sufficiently large number $(N_1 + N_2)$ of control volumes (3600–28 000) is applied for all our calculations; see the discussion in Sec. VI.

We consider two cases of periodic heating on the surface $z = 0$, where we apply (a) a heat flux boundary condition, or (b) a temperature boundary condition. For case (a), we fix the heat flux through the surface at $J(0,t) = J_{\max}\cos(2\pi f t)$ and calculate the corresponding $\Delta T_{\max}$ at the surface. For case (b), we fix the temperature on the surface at $T(0,t) = \Delta T_{\max}\cos(2\pi f t)$ and calculate the corresponding $J_{\max}$ at the surface. For both cases, we employ conservation of energy to calculate the temperature profile of the semi-infinite solid

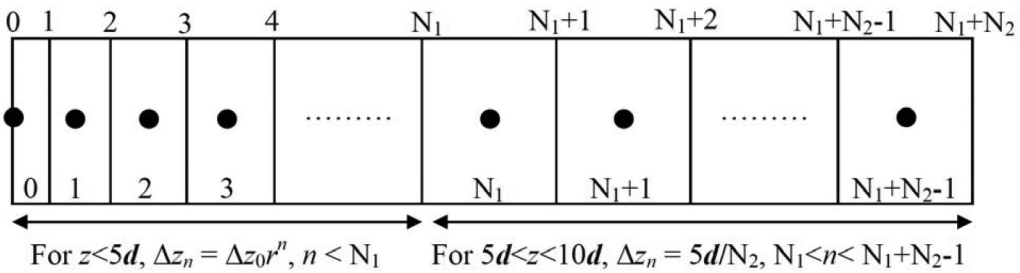

FIG. 2. The discretization scheme used in the derivation of the effective thermal conductivity at high heating frequencies. For $z < 5\boldsymbol{d}$, the nth control volume increases with z and given by $a_n = a_0 r^n$. For $5\boldsymbol{d} < z < 10\boldsymbol{d}$, the size of the control volumes is constant.

under periodic heating,

$$C\frac{\partial}{\partial t}T(z,t) = -\frac{\partial}{\partial z}J(z,t). \tag{15}$$

We use a control-volume formulation and a finite-difference formulation to numerically solve Eq. (15), for cases (a) and (b), respectively. Note that we apply nonlocal heat flux [Eq. (7)] or nonlocal gradient of heat flux [Eq. (9)] in solving Eq. (15); thus Eq. (15) is not a local equation.

V. MODIFIED CALLAWAY MODEL

To gain insights into the reduction of the apparent thermal conductivity at high frequencies, we compare calculations of the nonlocal theory to calculations of a modified Callaway model [15,29], which we adopted from Morelli and coworkers [30]. The modified Callaway model is based on the Debye-Callaway formalism with a separate treatment of the longitudinal and transverse phonon modes. We approximate the cutoff frequencies from the acoustic phonons at the zone boundary along [100]. Our expressions of the modified Callaway model differ slightly from those of Morelli *et al.* [30], since we allow mode conversion between longitudinal and transverse phonons for the normal three-phonon processes. Our expressions are listed below:

$$\Lambda = \Lambda_L + 2\Lambda_T,$$

$$\Lambda_L = \frac{1}{3}C_L T^3 (I_{L1} + \beta I_{L2}), \tag{16a}$$

$$\Lambda_T = \frac{1}{3}C_T T^3 (I_{T1} + \beta I_{T2}),$$

$$\beta = \left(\frac{I_{L2} + 2I_{T2}}{I_{L3} + 2I_{T3}}\right), \tag{16b}$$

$$I_{L1} = \int_0^{\theta_L/T} \frac{\tau_C^L(x)\, x^4 e^x dx}{(e^x - 1)^2}, \tag{16c}$$

$$I_{L2} = \int_0^{\theta_L/T} \frac{\tau_C^L(x)\, x^4 e^x dx}{\tau_N^L(x)(e^x - 1)^2}, \tag{16d}$$

$$I_{L3} = \int_0^{\theta_L/T} \frac{\tau_C^L(x)\, x^4 e^x dx}{\tau_N^L(x)\,\tau_R^L(x)(e^x - 1)^2}, \tag{16e}$$

$$C_{L(T)} = \frac{k_B^4}{2\pi^2\hbar^3 v_{L(T)}}, \tag{16f}$$

where $x = \hbar\omega/k_B T$ is the normalized phonon frequency, $\hbar$ is the Planck constant, ω is the frequency of phonons, k_B is the Boltzmann constant, T is the temperature, θ_L is the cutoff frequency for longitudinal phonons, v_L is the speed of sound for longitudinal phonons, and the subscripts and superscripts L denote longitudinal phonons. τ_C is defined as $1/\tau_C = 1/\tau_R + 1/\tau_N$; $1/\tau_R = 1/\tau_U + 1/\tau_I + 1/\tau_B$, where τ_U, τ_I, and τ_B denote the relaxation times for umklapp scattering, Rayleigh scattering due to impurities in the crystals, and boundary scattering, respectively. The corresponding integrals I_{T1}, I_{T2}, and I_{T3} have the same expressions as in Eq. (16), except that the cutoff frequency and relaxation times are for transverse phonons represented by subscripts and superscripts T.

We deviate from the approach of Ref. [30] and substitute a high-temperature expression for the scattering rate of the N process $\tau_N^{-1} = B_N\omega^2 T$. For simple crystals, we fix the relative anharmonic scattering strengths of umklapp and normal processes, B_U and B_N, by ratios of the phonon velocities, Grüneisen constants, and cutoff frequencies, and obtain absolute values of the anharmonic scattering strengths from fits to the bulk thermal conductivities. For crystals with compositional disorder, i.e., alloys, we assume a virtual crystal and use the average values of volume, mass, speeds of sound, cutoff frequencies, and thermal conductivities. We fit calculations of the modified Callaway model to the thermal conductivity of the virtual crystals to derive the anharmonic scattering strengths B_U and B_N. We calculate the strength of Rayleigh scattering in the alloys using the dimensionless parameters Γ_{mass} and Γ_{bond} that we previously derived; see Eqs. (1a) and (1b) of Ref. [31], that describe the strength of phonon scattering by mass disorder and bond disorder, respectively. We point out that this form of Rayleigh scattering strength is likely to be incorrect [32] since the scattering strength is not proportional to phonon density of states, as required by the first-order perturbation theory [33]. However, we continue to use this incorrect form of Rayleigh scattering strength, because, in this paper, the purpose of the Callaway model is only to systematically generate a wide range of phonon mean-free paths. Since we compare calculations of the nonlocal theory and the Callaway model using *exactly identical* distributions of phonon mean-free paths, our conclusions should not be affected by the exact forms of the scattering strengths used in the model. The parameters that we used are summarized in Tables I and II.

We define the mean-free paths of phonons by taking into consideration both direct retardation to heat conduction by the resistive scattering mechanisms (U process, Rayleigh scattering, and boundary scattering) and the indirect retardation by the N process,

$$\tau = \tau_C + \beta\tau_C/\tau_N, \tag{17a}$$

$$\ell = v\tau = v(\tau_C + \beta\tau_C/\tau_N). \tag{17b}$$

TABLE I. The cutoff temperature, θL and θT, speed of sounds, vL and vT, and the parameter Γ for Rayleigh scattering of Si, Ge, and Si0.9Ge0.1. For the crystals, the parameter Γ_{mass} is derived by assuming natural isotope composition.

Materials	θ_L (K)	θ_T (K)	v_L (m s^{-1})	v_L (m s^{-1})	Γ_{mass}	Γ_{bond}
Si	591	215	8440	5850	2.0×10^{-4}	0
Ge	343	114	4910	3540	5.9×10^{-4}	0
$Si_{0.5}Ge_{0.5}$	467	165	6670	4690	0.20	0.03

TABLE II. The fitted values of Grüneisen constants, γ_L and γ_T, and the corresponding strengths of anharmonic scattering, B_U and B_N, of Si, Ge, and $Si_{0.9}Ge_{0.1}$ derived using our approach.

Materials	γ_L	γ_T	$B_U^L(\mathrm{s\,K^{-1}})$	$B_U^T(\mathrm{s\,K^{-1}})$	$B_N^L(\mathrm{s\,K^{-1}})$	$B_N^T(\mathrm{s\,K^{-1}})$
Si	1.1	0.60	6.1×10^{-20}	1.7×10^{-19}	1.5×10^{-19}	2.2×10^{-19}
Ge	1.0	0.70	1.1×10^{-19}	3.0×10^{-19}	2.7×10^{-19}	3.5×10^{-19}
$Si_{0.5}Ge_{0.5}$	1.1	0.70	6.8×10^{-20}	1.9×10^{-19}	1.7×10^{-19}	2.4×10^{-19}

Mingo *et al.* [21] suggested that the frequency dependence could be due to omission of harmonic phonons, which they defined as phonons with anharmonic mean-free paths larger than $3\boldsymbol{d}$. To test whether the frequency dependence of thermal conductivity is due to insensitivity of the measurements to harmonic phonons, we also define an anharmonic mean-free path $\boldsymbol{\ell}_{\mathrm{anh}}$ that takes into consideration only the anharmonic scattering,

$$\boldsymbol{\ell}_{\mathrm{anh}} = v\left[\left(\tau_U^{-1} + \tau_N^{-1}\right)^{-1} + \beta\tau_C/\tau_N\right]. \tag{18}$$

For illustration purposes, we plot in Fig. 3 $I_L(z)$ of longitudinal phonons in bulk Si, a 200-nm Si thin film, and bulk $Si_{0.5}Ge_{0.5}$ alloy using the relaxation times described here. From Fig. 3, the distances z at which $1/e = 37\%$ of the flux of longitudinal phonons remains unscattered are 145, 65, and 1 nm for Si, the Si thin film, and the $Si_{0.5}Ge_{0.5}$ alloy, respectively.

In this paper, we employ the modified Callaway model to calculate the thermal conductivity of a series of hypothetical Si crystals. To modify the spread of phonon mean-free paths in the hypothetical Si, we vary the parameter Γ for Rayleigh scattering from $\Gamma = 2 \times 10^{-4}$ to $\Gamma = 2$. The total relaxation time and the mean-free path of phonons are then calculated using Eq. (17). The same total relaxation time is applied in our calculations of the nonlocal theory. We emphasize that since we employ exactly identical phonon dispersion and scattering in calculations of both models, our conclusions do not hinge on the accuracy of the modified Callaway model.

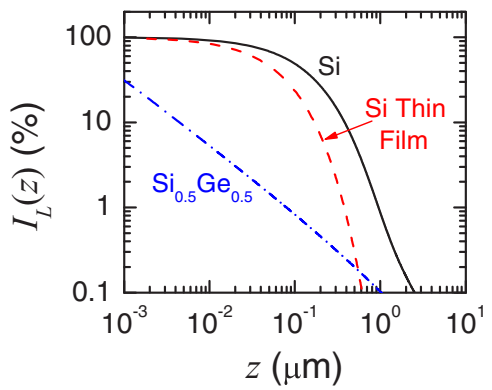

FIG. 3. (Color online) The percentage of flux of unscattered longitudinal phonons $I_L(z)$ in bulk Si (solid lines), a 200-nm Si thin film (dashed lines), and bulk $Si_{0.5}Ge_{0.5}$ alloy (dash-dotted lines). z is the distance in the direction of temperature gradient.

VI. RESULTS

We solve the nonlocal theory for a semi-infinite solid using (a) heat flux and (b) temperature boundary conditions, and plot the calculated results as a function of the number of control volumes and the heating frequency in Fig. 4. For alloys and low frequencies, we find that the normalized amplitudes and relative phases calculated for cases (a) and (b) yield identical results when the number of control volumes is sufficiently high; the ratios $J_{\max}/T_{\max}$ are identical irrespective of whether Dirichlet [case (a)] or Neumann [case (b)] boundary conditions are applied. Since we apply different numerical schemes [the finite-volume formulation for case (a) and the finite-difference formulation for case (b)] and use different equations [Eq. (7) for case (a) and Eq. (9) for case (b)], the agreement between calculations of both cases supports the validity of the derived model. However, for crystals at high frequencies, the calculated values using the two different boundary conditions differ, irrespective of the number of control volumes applied. We do not know the origins of this discrepancy. We thus omit three calculations with discrepancies between cases (a) and (b) that are greater than 15%.

To test whether ballistic or harmonic phonons are responsible for the observed frequency dependence of thermal conductivity, we compare the nonlocal calculations of Λ_{amp}, Λ_{out}, and Λ_{in} of the hypothetical Si with calculations using the modified Callaway model that omits contribution from either ballistic ($\boldsymbol{\ell} > 2\boldsymbol{d}$) or harmonic ($\boldsymbol{\ell}_{\mathrm{anh}} > 3\boldsymbol{d}$) phonons; see Fig. 5. Here, we follow Mingo *et al.* [21] to define the harmonic phonons as phonons that are not scattered by anharmonic processes within a cutoff length η, i.e., phonons with $\boldsymbol{\ell}_{\mathrm{anh}} > \eta$, where $\boldsymbol{\ell}_{\mathrm{anh}}$ is the mean-free path considering on the anharmonic scattering. For the ballistic case, we adjust the cutoff length ($\boldsymbol{\ell} > 2\boldsymbol{d}$) to get good agreement between calculations obtained using both models, while for the harmonic case, we use the fitted cutoff value ($\boldsymbol{\ell}_{\mathrm{anh}} > 3\boldsymbol{d}$) by Mingo *et al.* [21]. We find that for alloys, Callaway calculations omitting the ballistic phonons ($\boldsymbol{\ell} > 2\boldsymbol{d}$) fit the calculations of the nonlocal theory well for all effective thermal conductivities Λ_{amp}, Λ_{out}, and Λ_{in}, while Callaway calculations omitting the harmonic phonons ($\boldsymbol{\ell}_{\mathrm{anh}} > 3\boldsymbol{d}$) severely overestimate the frequency dependence; see Fig. 5. This result suggests that the frequency dependence of apparent thermal conductivity of alloys could be adequately approximated by the assumption that ballistic phonons do not contribute to apparent heat conduction, as we previously asserted [15].

Interestingly, we find that Λ_{out} is almost independent of f when Γ is small; see Fig. 5(b). The reason is that while the amplitude of the calculated heat flux reduces with increasing

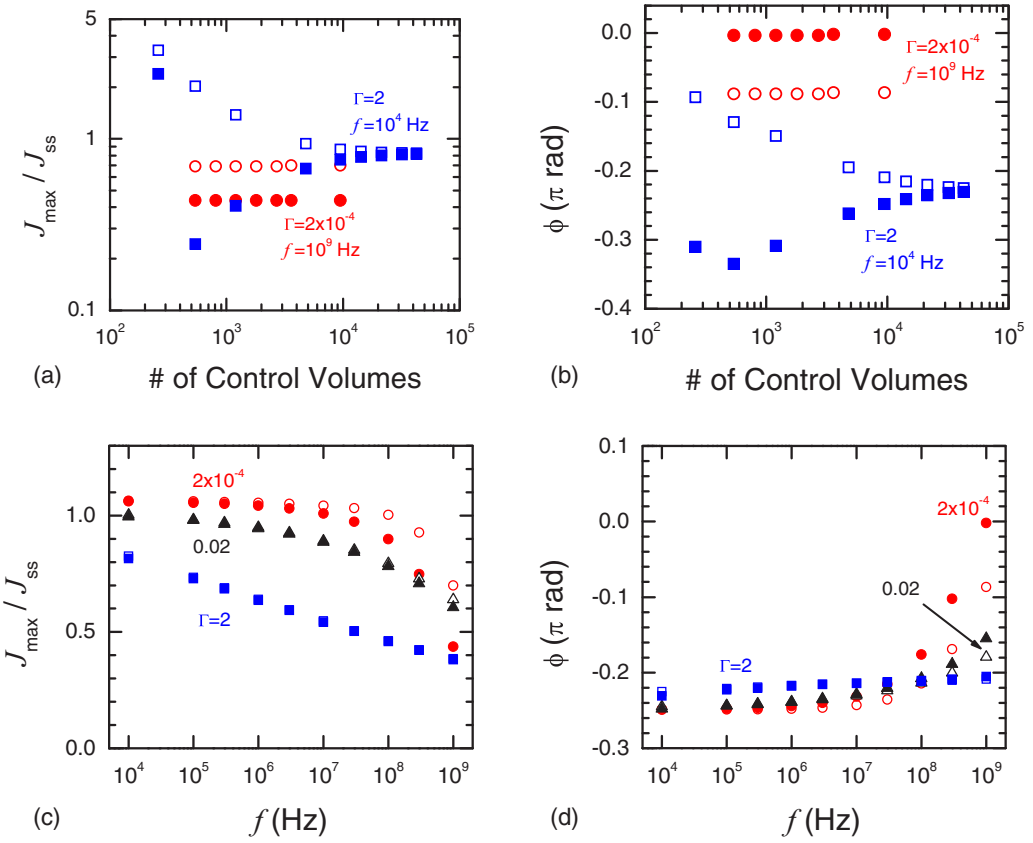

FIG. 4. (Color online) (a),(b) The normalized amplitude (a) and relative phase (b) of heat flux calculated under prescribed heat flux (case A, open symbols) and prescribed temperature (case B, solid symbols) at the surface, as a function of total number of control volumes in the calculations, for two hypothetical Si with different Rayleigh scattering strengths Γ. For a high Γ at a low heating frequency (squares, $\Gamma = 2$, $f = 10^4$ Hz), calculations for cases A and B converge after sufficient numbers of control volumes. For a crystal at a high heating frequency (circles, $\Gamma = 2 \times 10^{-4}$, $f = 10^9$ Hz), calculations for cases A and B do not converge. (c, d) The normalized amplitude (c) and relative phase (d) of the calculated heat flux as a function of the heating frequency f, for the hypothetical Si with different Γ, as labeled. If calculations with prescribed heat flux (case A, open symbols) and with prescribed temperature (case B, solid symbols) differ by more than 15%, the calculations are omitted in following analysis.

frequency, see Fig. 4(c), the relative phase diminishes; see Fig. 4(d). Due to the compensating effects of the diminishing amplitude and phase, Λ_{out} is almost independent of f. Since TDTR measurements are mostly sensitive to Λ_{out}, this finding is consistent with the lack of frequency dependence observed in prior TDTR measurements of crystals.

To better illustrate our results, we plot nonlocal calculations of the ratio of Λ_{amp}, Λ_{out}, and Λ_{in} at $f = 10$ MHz to that at

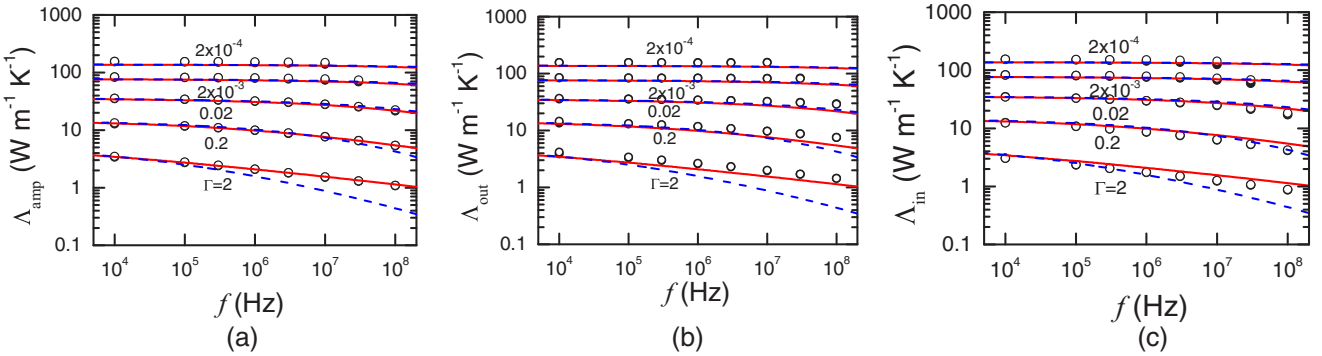

FIG. 5. (Color online) The apparent thermal conductivity calculated from (a) the amplitude Λ_{amp}, (b) the out-of-phase Λ_{out}, and (c) the in-phase Λ_{in} of heat flux calculated under prescribed heat flux (case A, open circles) and prescribed temperature (case B, solid circles), as a function of the heating frequency f. The materials considered are hypothetical Si with different parameter Γ for Rayleigh scattering, as labeled. The solid and dashed lines are the corresponding calculations using the modified Callaway model, assuming ballistic ($\ell > 2d$) and harmonic ($\ell_{anh} > 3d$) phonons do not contribute to heat conduction, respectively.

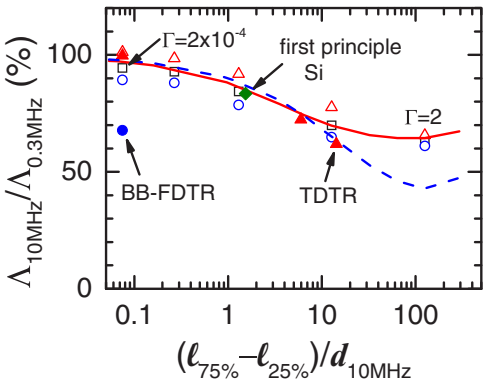

FIG. 6. (Color online) Ratios of the apparent thermal conductivity of the hypothetical Si at 10 MHz ($\Lambda_{10\,\mathrm{MHz}}$) to that at 0.3 MHz ($\Lambda_{0.3\,\mathrm{MHz}}$) calculated from the amplitude (open squares), the out-of-phase (open triangles) and in-phase (open circles) of heat flux using the nonlocal theory, as a function of spread of the mean-free paths of phonons ($\boldsymbol{\ell}_{75\%} - \boldsymbol{\ell}_{25\%}$) in the hypothetical Si normalized by the thermal penetration depth at 10 MHz ($d_{10\,\mathrm{MHz}}$). The solid triangles are TDTR measurements [15,29] on Si and SiGe, plotted as a function of calculated $(\boldsymbol{\ell}_{75\%} - \boldsymbol{\ell}_{25\%})/d_{10\,\mathrm{MHz}}$. The solid circle is derived from BB-FDTR measurements from Ref. [18]. The solid and dashed lines are calculations using the modified Callaway model, assuming ballistic ($\boldsymbol{\ell} > 2\boldsymbol{d}$) and harmonic ($\boldsymbol{\ell}_{\mathrm{anh}} > 3\boldsymbol{d}$) phonons do not contribute to heat conduction, respectively. The solid diamond is derived from first-principle calculations [19], assuming that ballistic phonons ($\boldsymbol{\ell} > 2\boldsymbol{d}$) do not contribute to heat conduction.

$f = 0.3$ MHz in Fig. 6; the frequencies represent the upper and lower frequency limits in most TDTR measurements. We plot the ratio as a function of the normalized spread of phonon mean-free paths $(\boldsymbol{\ell}_{75\%} - \boldsymbol{\ell}_{25\%})/d_{10\,\mathrm{MHz}}$ used in the calculations. Here, $\boldsymbol{\ell}_{75\%}$ and $\boldsymbol{\ell}_{25\%}$ are the mean-free paths of phonons when the accumulated thermal conductivities (i.e., sum of the thermal conductivity by phonons with zero to the specific mean-free path) are 75% and 25% of the steady-state value respectively, while $d_{10\,\mathrm{MHz}}$ is the thermal penetration depth $\boldsymbol{d}$ at 10 MHz. The rationale for the choice of the x axis is that the reduction of the apparent thermal conductivity depends strongly on the spread of the phonon mean-free paths of phonons; the wider the spread of the mean-free paths, the stronger is the reduction of the thermal conductivity at high frequencies. Using our modified Callaway model $(\boldsymbol{\ell}_{75\%} - \boldsymbol{\ell}_{25\%})/d_{10\,\mathrm{MHz}}$ equals 0.075 and 125 for $\Gamma = 2 \times 10^{-4}$ (Si) and $\Gamma = 2$ respectively, while first-principle calculations [20] of Si give $(\boldsymbol{\ell}_{75\%} - \boldsymbol{\ell}_{25\%})/d_{10\,\mathrm{MHz}} = 1.5$.

In Fig. 6, we also plot calculations of the ratios of the effective thermal conductivities at $f = 10$ MHz and $f = 0.3$ MHz using the modified Callaway model, by excluding either ballistic ($\boldsymbol{\ell} > 2\boldsymbol{d}$) or harmonic ($\boldsymbol{\ell}_{\mathrm{anh}} > 3\boldsymbol{d}$) phonons for the respective frequencies. Comparison of the calculations of the nonlocal and Callaway models in Fig. 6 clearly illustrates that reductions in the Λ at high frequencies could be well approximated, over a wide range of spread of phonon mean-free paths, by the omission of ballistic phonons with $\boldsymbol{\ell} > 2\boldsymbol{d}$.

In Fig. 6, we also plot the TDTR [14,26] and BB-FDTR [18] measurements of natural Si and SiGe alloys, as a function of the normalized spread of phonon mean-free paths $(\boldsymbol{\ell}_{75\%} - \boldsymbol{\ell}_{25\%})/d_{10\,\mathrm{MHz}}$ *calculated* using the modified Callaway model. We note that since the accuracy of the phonon mean-free paths assumed in our Callaway model is disputable, the comparison does not provide insights into the accuracy of the measurements. We find that the nonlocal calculations agree well with the prior TDTR measurements [15,29] on natural Si and SiGe. Notably, the reduction of the thermal conductivity measured by BB-FDTR [18] on natural Si is significantly more pronounced compared to the TDTR measurements. Comparison with our nonlocal calculations indicates that the discrepancy between the TDTR and BB-FDTR measurements on Si is not due to different ways the data are analyzed in TDTR and BB-FDTR, since the disparity between derived Λ_{amp}, Λ_{out}, and Λ_{in} values is substantially smaller than the difference between the TDTR and BB-FDTR measurements. Potential problems of the BB-FDTR measurements [18] are discussed by Wilson and Cahill in Ref. [22].

VII. CONCLUSION

In summary, we present a nonlocal theory that governs heat transfer at high frequencies, e.g., in TDTR and BB-FDTR measurements, and high-frequency electronic devices. Comparison of calculations of the nonlocal theory and a modified Callaway model suggests that while the amplitude of heat conduction at high frequencies can be conveniently approximated using an effective thermal conductivity reduced by omitting ballistic phonons with $\boldsymbol{\ell} > 2\boldsymbol{d}$, the relative phase between temperature and heat flux oscillation, especially for pure crystals at high frequencies, is no longer $\pi/4$ and cannot be easily estimated. Thus, simple interpretation of omitting ballistic phonons with mean-free paths larger than the penetration depth is only a good approximation for measurements on alloys and is not justified for TDTR and BB-FDTR measurements on pure crystals, since the measurements also depend on the phase of the induced temperature oscillations.

We note the limitations of our nonlocal model. (1) Our model is only valid when the size of the heat source is significantly larger than the mean-free paths of the heat carriers, and thus it cannot explain the spot size dependence of measurements of apparent thermal conductivity. (2) In our model, it is assumed that the interfacial thermal resistance is negligible and phonons are thermalized at the interfaces. While this is a reasonable assumption for high-energy phonons at room temperature, low-energy phonons might not be scattered at the interfaces [26,34], and thus not thermalized. As a result, the apparent thermal conductivity measured at high frequencies could be dominated by the interfacial effects [22], especially at low temperatures. In such cases, a much more pronounced frequency dependence could be observed.

ACKNOWLEDGMENTS

We thank R. Wilson for useful discussion. This material is based upon work supported by the Singapore Ministry of Education Academic Research Fund Tier 2, under Award No. MOE2013-T2-2-147.

[1] T. Klitsner, J. E. VanCleve, H. E. Fischer, and R. O. Pohl, Phys. Rev. B **38**, 7576 (1988).
[2] K. Schwab, E. A. Henriksen, J. M. Worlock, and M. L. Roukes, Nature (London) **404**, 974 (2000).
[3] P. G. Sverdrup, S. Sinha, M. Asheghi, S. Uma, and K. E. Goodson, Appl. Phys. Lett. **78**, 3331 (2001).
[4] H. Y. Chiu, V. V. Deshpande, H. W. C. Postma, C. N. Lau, C. Mikó, L. Forró, and M. Bockrath, Phys. Rev. Lett. **95**, 226101 (2005).
[5] M. E. Siemens, Q. Li, R. Yang, K. A. Nelson, E. H. Anderson, M. M. Murnane, and H. C. Kapteyn, Nat. Mater. **9**, 26 (2010).
[6] L. G. C. Rego and G. Kirczenow, Phys. Rev. Lett. **81**, 232 (1998).
[7] G. Chen, Phys. Rev. Lett. **86**, 2297 (2001).
[8] G. Chen, Phys. Rev. B **57**, 14958 (1998).
[9] N. Mingo and D. A. Broido, Phys. Rev. Lett. **95**, 096105 (2005).
[10] J. Wang and J.-S. Wang, Appl. Phys. Lett. **88**, 111909 (2006).
[11] B. C. Larson, J. Z. Tischler, and D. M. Mills, J. Mater. Res. **1**, 144 (1986).
[12] G. D. Mahan and F. Claro, Phys. Rev. B **38**, 1963 (1988).
[13] A. J. Minnich, G. Chen, S. Mansoor, and B. S. Yilbas, Phys. Rev. B **84**, 235207 (2011).
[14] D. Ding, X. Chen, and A. J. Minnich, Appl. Phys. Lett. **104**, 143104 (2014).
[15] Y. K. Koh and D. G. Cahill, Phys. Rev. B **76**, 075207 (2007).
[16] X. Liu, J. L. Feldman, D. G. Cahill, R. S. Crandall, N. Bernstein, D. M. Photiadis, M. J. Mehl, and D. A. Papaconstantopoulos, Phys. Rev. Lett. **102**, 035901 (2009).
[17] H.-S. Yang, D. G. Cahill, X. Liu, J. L. Feldman, R. S. Crandall, B. A. Sperling, and J. R. Abelson, Phys. Rev. B **81**, 104203 (2010).
[18] K. T. Regner, D. P. Sellan, Z. Su, C. H. Amon, A. J. H. McGaughey, and J. A. Malen, Nat. Commun. **4**, 1640 (2013).
[19] A. Ward and D. A. Broido, Phys. Rev. B **81**, 085205 (2010).
[20] K. Esfarjani, G. Chen, and H. T. Stokes, Phys. Rev. B **84**, 085204 (2011).
[21] C. A. da Cruz, W. Li, N. A. Katcho, and N. Mingo, Appl. Phys. Lett. **101**, 083108 (2012).
[22] R. B. Wilson and D. G. Cahill, Nat. Comm. **5**, 5075 (2014).
[23] R. B. Wilson, J. P. Feser, G. T. Hohensee, and D. G. Cahill, Phys. Rev. B **88**, 144305 (2013).
[24] A. J. Minnich, J. A. Johnson, A. J. Schmidt, K. Esfarjani, M. S. Dresselhaus, K. A. Nelson, and G. Chen, Phys. Rev. Lett. **107**, 095901 (2011).
[25] K. F. Riley, M. P. Hobson, and S. J. Bence, *Mathematical Methods for Physics and Engineering* (Cambridge University Press, Cambridge, England, 2006).
[26] Y. K. Koh, Y. Cao, D. G. Cahill, and D. Jena, Adv. Funct. Mater. **19**, 610 (2009).
[27] D. G. Cahill, Rev. Sci. Instrum. **75**, 5119 (2004).
[28] H. S. Carslaw and J. C. Jaeger, *Conduction of Heat in Solids* (Oxford University Press, Oxford, 1959).
[29] Y. K. Koh, Ph.D. thesis, University of Illinois, 2010.
[30] D. T. Morelli, J. P. Heremans, and G. A. Slack, Phys. Rev. B **66**, 195304 (2002).
[31] Y. K. Koh, C. J. Vineis, S. D. Calawa, M. P. Walsh, and D. G. Cahill, Appl. Phys. Lett. **94**, 3 (2009).
[32] R. Wilson (private communication).
[33] S.-i. Tamura, Phys. Rev. B **27**, 858 (1983).
[34] M. N. Luckyanova *et al.*, Science **338**, 936 (2012).